Micro-Solvation of Propofol in Propylene Glycol-Water Binary Mixtures: Molecular Dynamics Simulation Studies

Anupama Sharma, Vishal Kumar, and Sudip Chakraborty*

Department of Computational Sciences, School of Basic Sciences, Central University of Punjab, Bathinda, India-151401

E-mail: sudip.chakraborty@cup.edu.in*

Abstract

The water micro-structure around propofol plays a crucial role in controlling their solubility in the binary mixture. The unusual nature of such water micro-structure can influence both translational and reorientational dynamics, as well as the water hydrogen bond network near propofol. We have carried out the all atom molecular dynamics (MD) simulations of five different compositions of propylene glycol (PG): water binary mixture containing propofol (PFL) molecules to investigate the differential behavior of water micro-solvation shells around propofol, which is likely to control the propofol solubility. It is evident from the simulation snapshots for various composition that the PG at high molecular ration favors the water cluster and extended chainlike network that percolates within the PG matrix, where the propofol is in the disperse state. We estimated the radial distribution function indicates higher ordered water micro-structure around propofol for high PG content, as compared to the lower PG content

in the PG:Water mixture. So, the hydrophilic propylene glycol regulates the stability of water micro-network around propofol and their solubility in the binary mixture. We observed the translational and rotational mobility of water belonging to the propofol micro-solvation shell is hindered for high propylene glycol content, and relaxed towards the low propylene glycol molecular ration in the PG:Water mixture. It has been noticed that the structural relaxation of the hydrogen bond formed between the propofol and the water molecules present in the propofol micro-solvation shell for all five compositions, is found slower for high PG content, and becomes faster on the way to low PG content in the mixture. Simultaneously, we calculated the intermittent residence time correlation function of the water molecules belonging to the micro-solvation shell around the propofol for five different compositions, and found a faster short time decay followed up with a long time components. Again, the origin of such long time decay primarily from the structural relaxation of the micro-solvation shell around the propofol, where the high propylene glycol content shows the slower structural relaxation that turns faster as the propylene glycol content approaches to the other end of the compositions. So, our studies showed that the slower structural relaxation of the micro-solvation shell around propofol for high propylene glycol molecular ration in the PG:Water mixture, correlate well with the extensive ordering of water micro-structure and restricted water mobility, facilitates the dissolution process of propofol in the binary mixture.

Introduction

Bioavailability of poorly soluble drugs pose a significant challenge owning to their stability and formulation.[1] Water solubility is one of the key parameters that influences the drugs ability to dissolve in bodily fluids and being directly absorbed.[2] Hence, improving drug bioavailability has led to constant growth of an array of delivery mechanisms and solution preparation in modern drug development.[1,3,4] In recent years, studies have shown that water molecules present at the interface between the drug and the receptor plays a crucial role in the binding process.[5,6] Additionally, water molecules present in the vicinity of the receptor can also influence the activity of anesthetics both local and general.[7] This underscores the importance of understanding the interactions between anesthetics and water molecules at first in order to better understand and improve the efficacy of these drugs. Preferential solvation study of drug molecules in alcohol-water,[8,9] glycol-water cosolvent mixtures,[10–12] ionic liquid-water cosolvent composition[13,14] have been reported. Several aqueous alcohol mixtures of varying composition, temperature and pressure have been studied for industrial importance too.[15–18]

Propofol (2,6-diisopropylphenol) is a general intravenous anesthetic molecule, developed by John Baird Glen in search of safer and effective anesthesia.[19] It is widely used due to its rapid onset and quick recovery.[20] Studies suggest propofol pose its action on presynaptic receptors, it activates $GABA_AR$ function,[21–23] inhibits voltage gated sodium ion channels.[24] It is a phenolic compound with two isopropyl group ortho to sterically hindered hydroxyl group. Steric hindrance due to the presence of two alkyl group obstruct the formation of hydrogen bonds in aqueous media. Thus, propofol is merely soluble in aqueous solution with octanol:water partition coefficient reported as 6,761:1.[25] Emulsion based formulation are available as Diprivan® which is composed of soyabean oil, glycerol and purified egg phosphatide for intravenous use in clinic.[26] Though, they are found to have minor incidence

of postoperative nausea and vomiting, risk associated with long term uses such as pain on injection, hyperlipidemia, poor physical stability, bacterial contamination after exposure to air are not uncommon[27 28 29 30 31 32].[33] Considering the clinical potency, studies persisted in search for safer and efficacious vehicles[34].[35,36]

Propylene glycol is an industrially important amphiphilic diol[37 38,39].[40] It is a viscous liquid with the ability to depress water crystallization and melting which makes its use in antifreeze solutions.[38,39] The high specific heat capacity of the propylene glycol-water (PG−Water) mixture gives its potential application in gasifying liquefied natural gas.[37] It is Known for its lipid destabilizing role,[40] and used as a chemical enchancer in topical formulation to cure skin disorders.[41–43] It has gained interest in cell preservation for its cryoprotectant ability in solutions.[44] It is considered safe for administrative purposes and hence used to dissolve several drug molecules in drug administrative formulation.[45,46] Several experimental investigation for the aqueous propylene-glycol water mixtures have been reported[47 48 49].[50] However, the understanding of the solution for the prevention of water crystallization was the main principal in the works[47].[49] Considering the safety, propylene glycol is the most widely used cosolvent in the design and development of liquid medicines.[51] It has been used as a testing solvent model for the solubility of several drug molecules in experiments[52].[53] Jimenez et al. studied the effect of propylene glycol water mixture concentration on three pharmaceutical salts of varied pH values.[54] The driving mechanism for the solubility of drug meloxicam in water-rich composition was due to disturbed water-structure near the drug and is entropic in nature, while for PG-rich it is enthalpic due to better solvation.[12] Gao and Olsen Studied the extent of drug acetaminophen release in aqueous NaCl solution, suggesting interplay between interaction forces with solvent molecules and with other drugs plays a role.[55] Trapani et al. studied solubility of propofol in 1:1 v/v propylene glycol:water binary solution. They found the mixture was able to solubilize 10mg/ml of propofol with induction time and duration of action comparable to that of Diprivan®.[35]

Solubilization of propofol in aqueous solution have been reported in several experimental investigation[56–59 60 36].[61] Dwyer et al. studied propofol in the aqueous solutions of Pluronics where increased propofol in solution induces micelle formation and propofol is likely to be solubilized in the core.[56] Cho et al. studied the microemulsion of propofol for intravenous injection formulated using aqueous nonionic surfactants, poloxamers and polyethylene glycol 660 hydroxystearate. This new formulation was found to cause considerably low histamine release compared to the macroemulsion earlier reported.[57] NMR study of propofol in nonionic surfactants reveals higher diffusion coefficient of propofol than that of surfactant caused by the partitioning of propofol between swollen micelles and the aqueous solution.[58] Vibrational sum frequency generation (VSFG) technique was used to understand the dissociation as well as hydration of propofol at the water interface under different pH conditions.[59] Duration of unresponsivnes to propofol ingestion combined with remifentanil-fentanyl anesthetic have been reported using combined Pharmacokinetic Pharmacodynamic Models.[60] Drug delivery potency of cyclodextrin molecules with propofol have been tested and found to improve its pharmacokinetic and pharmacodynamic properties at blood brain barrier.[36] Mass-resolved excitation spectroscopy suggests the fromation of homodimer and its single hydrogen bond bridge propofol dimer complex. Further, results suggest strong CH-π interaction with weak hydrogen bonds between the molecules and water.[61] Interestingly, the water network near propofol plays an important role in the binding of general anesthetic to proteins. Using NMR spectroscopy, Wang et. al. have reported that the critical amount of hydration water is absolutely essential for anesthetic - protein binding.[62]

Molecular dynamics (MD) simulation studies can assist to solve many unsolved issues regarding the in-depth insight of molecular interactions and the nature of the dynamics of water near propofol at the microscopic level. In recent past, Klein and coworkers have conducted MD simulation studies to investigate the mechanistic aspects of general anesthetics isoflurane and propofol action on prokaryotic pentameric channel GLIC.[63] They reported

that both the molecules shows pore inhibition mechanism at the micromolar concentrations, and have a higher affinity in the unoccupied pore as compared with the allosteric site. In 2018, Wang et. al. have reported various propofol binding sites in NaChBac using molecular docking and MD simulation studies.[24] However, Henin et. al. have used alchemical free energy perturbation (FEP) technique to calculate affinities for isoflurane binding to apoferritin, which compared well to experiment.[64] Further, Tang and coworkers have reported the nature and locations of halothane interactions using flexible ligand docking to their model of the $\alpha_4\beta_2$ nAChR in an open conformation.[65] The binding free energy calculation shows that halothane binds with low affinity to most sites. So, the atomistic level investigations including propofol and several other anesthetic molecules have begun to be more prominent in recent years by employing the MD simulation technique.[66] In early research work, Koubi et. al. have shown the presence of anesthetic molecules alters the membrane structural properties.[67] They observed the presence of the molecule led to a large perturbation of the electrostatic potential across to the membrane interface, as well as the substantial increase in the microscopic viscosity of the lipid core compared with the pure lipid bilayer. The observed perturbations of the lipid membranes in the presence of anesthetics are showing the difference in their physiological effects as compared to the non-immobilizers. Interaction of anesthetic molecules propofol and fentanyl with lipid bilayer (DOPC and DPPC) have been studied using atomistic simulation.[68] The increased content of propofol in DPPC bilayer causes the decrease in isothermal compressibility modulus along with decrease of melting temperature.[69] Umbrella sampling simulation studies suggests the partition of propofol into a gel DPPC phase is not favorable and it is mainly enthalpy driven at the polar region.[70] Ahmad et al. have conducted the coarse-grained simulation to study the propofol within the quaternary ammonium palmitoyl glycol chitosan (GCPQ) micelle solution and found a heterogenous distribution within the micellar population.[71] Importantly, the solubility of anesthetics in deep eutectic solvent have also been explored using theoretical calculations.[72]

Despite being widely used and studied, understanding the solvation processes of propofol in aqueous medium remains elusive and hasn't achieved the same degree of knowledge as aspects derived from pharmaceutical evolution. It is well accepted that the molecular aggregation / dissolution process is partially controlled by the nature of the water micro-structure around the propofol. So, the characterization of the micro-solvation shell of propofol can exploring the hidden truth that plays a vital role in determining the stability of the drug (propofol) solubilized in binary mixture is important. To the best of our knowledge, these facts have not been investigated in detail and require more attention. To investigate the differential behavior of water micro-solvation shells around propofol, we have performed atomistic molecular dynamics simulations of five different compositions of propylene glycol : water mixture containing propofol molecules. In this work, we have calculated various correlation functions including the ones that give information regarding the structural arrangement of molecules within the system including radial distribution function. Rotational correlation and mean squared displacement have been calculated to investigate the dynamics of water in the propofol micro-solvation shells for all five compositions, followed up with the dynamics of hydrogen bond formed between propofol and water molecules and the intermittent residence time correlation function. This article is organized as follows: Starting with the discussion of simulation and its methods that have been employed in the current study, including the force fields. The detailed investigation of structural and dynamical properties, as observed during the simulation has been reported in the form of snapshots followed by reporting the various correlation function analysis and their interpretation. In the last section, we will summarize the important findings from our study.

Methodology

System Setup and Simulation Details

Initially, we have constructed cubic simulation box containing propylene glycol-water binary mixture with propofol molecules for individual compositions using the GROMACS tools,[73,74] the approximate dimension and compositions are listed in table1. Where, we have opted seven propofol molecules for individual simulation system, and the S2 simulation setup is based on the experimental report by Trapani and co-workers,[35] along with other compositions (table 1). For Bulk water, a cubic box of 1054 water molecules was build separately. The CHARMM General Force Field (CGenFF) was used to obtained the propylene glycol parameters.[75,76] The CHARMM modified TIP3P water model was used to model the solvent,[77] and the CHARMM-consistent propofol parameters were taken from a recent study.[63] The simulation experiment on the constructed systems were initiated by removing the unfavorable contacts via steepest descent energy minimization. This was followed by a rapid equilibration at constant temperature (T = 300 K) and volume (NVT). Each NVT equilibration was carried out for 10 ns duration, followed up with a constant temperature (T = 300 K) and pressure (P = 1.0 atm), NPT simulation run for 20 ns. The final equilibration of the system was continued via a production run of 100 ns in the NPT ensemble, with simulated trajectories were stored at every 100 ps. Structural properties can be calculated from 100 ns NPT simulation. For investigating the coordination number, diffusion, hydrogen bond relaxation, residence time correlation and reorientational aspects of water molecules, a 1 ps resolution NVT run was further carried out for 10 ns duration. Additional, 5fs high resolution trajectory of 50 ps time was also generated to probe the ultrafast translational and dynamical aspects of water.

We were carried out all atom molecular dynamics (MD) simulations corresponds to the varied composition of propylene glycol:water binary mixtures with propofol (Table 1) using

the 2018.3 version of the parallel MD simulation package GROMACS.[73,74] In the whole course of simulations, the LINCS algorithm[78] was employed for bond constraints. Leap-frog integrator was used to solve Newton's equation of motion to generate the time reversible trajectory. Verlet cutoff scheme was used for neighbor list generation with a cutoff of 1.2 nm with every 10 step neighbor list update. A cut-off radius of 1.2 nm was used for all van der Waals interactions and standard long-range corrections have also been taken into consideration. The Long range electrostatic interactions were treated using the Particle Mesh Ewald (PME) method,[79,80] with cubic interpolation of the order of 4 and a fourier spacing of 0.16 nm. In our simulations, we employed 1.2 nm for the real space cutoff. Temperature coupling in the NVT and NPT runs were provided via a Velocity-Rescaling Thermostat[81,82] of relaxation time, 1.0 ps, where the velocities are scaled by a factor λ in order to attain desired temperature quickly. Velocity Rescale Thermostat is a modified Berendsen thermostat with a stochastic term added, that ascertain correct kinetic energy distribution has been achieved and proper canonical ensemble is generated.[81,82] Whereas, Pressure Coupling in the system was provided by Parrinello-Rahman Barostat[83,84] with a isotropic coupling constant of 1.0 ps and a compressibility factor of 4.5×10^{-5} bar^{-1}. All of the simulation boxes followed the three dimensional Periodic Boundary Conditions (3D PBC), with the 2fs time step of simulation. All of the images are produced using VMD.[85]

Table 1: Details of Molecular Dynamics Simulations of Propofol(PFL):Propylene Glycol(PG):Water Mixtures

System	PFL:PG:Water						
	PG	Water	PFL	f(V/V)	PG Slab(nm)	Water Slab(nm)	Box Dimension (nm)
S1	1033	2994	7	1.4	6×6×3.5	6×6×2.5	6×6×6
S2	886	3592	7	1.0	6×6×3	6×6×3	6×6×6
S3	738	4192	7	0.7	6×6×2.5	6×6×3.5	6×6×6
S4	590	4790	7	0.5	6×6×2	6×6×4	6×6×6
S5	148	6587	7	0.1	6×6×0.5	6×6×5.5	6×6×6

Result and Discussion

Structural Inspection : A molecular level heterogenity

The configurations of five different simulated systems at the beginning and at the the end of the simulation are displayed in figure 1. It is clear from the figure that the propofol in PG:Water binary mixture shows the modulation of structure formation and clustering with varying composition (table 1) during the nanosecond timescale of the simulation. The important notable feature from the figure 1 is that, as the simulation progresses, the segregation happens at the microscopic level differently as per their composition. This is in contrast to an almost zero segregation and distinct liquid composition at the beginning.

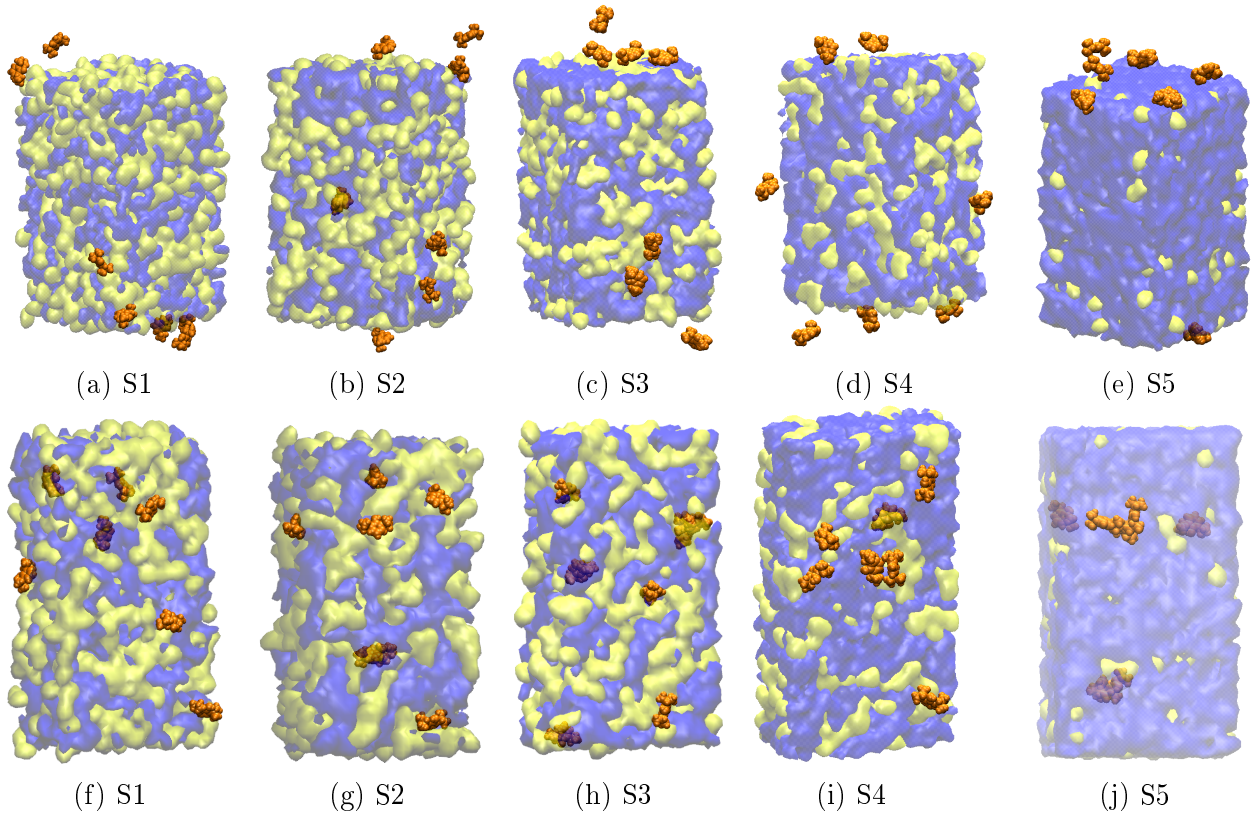

(a) S1 (b) S2 (c) S3 (d) S4 (e) S5

(f) S1 (g) S2 (h) S3 (i) S4 (j) S5

Figure 1: Snapshots of the configuration correspond to five different (table 1) simulated systems at the beginning (equilibrated Propylene Glycol:Water mixture and Propofol) and at the end of the simulation. Yellow and Blue color surface plot represents Propylene Glycol and Water molecules, whereas the Propofol molecules are represented by vdW plots with Brown color.

Several groups have recently been tried to unfold the microscopic interaction behavior of water and propylene glycol in solution[86,87] and reported water-PG interaction is more preferred in 30 mol% solution over PG-PG self interaction and the similar observation has been reported for 50 mol% solution.[87] Observations of water clustering behavior in presence of small amphiphilic molecules such as methanol, DMSO, Glycerol has long been known.[17,18,88]

It is evident from the beginning and end of the simulation snapshots for various composition that the propylene glycol at low molecular ration form clusters and tends to interact more with itself than with water, and in such case the propofol molecules shows a tendency

to form aggregate, which may reduce their solubility in PG:Water binary mixture (S5). Interestingly, at higher propylene glycol composition ratio (S1) the water in the binary mixture favors the extended chainlike[89] connectivity and the propofol prefers the dispersed state. In the system S2, the similar dispersion behavior of propofol has been observed as like S1, and the water molecules tend to form both cluster and chainlike networks[89] that percolate within the propylene glycol (PG) matrix. So, the higher propylene glycol vol/vol % ratio indicates the augmented tendency of the formation of chainlike water networks in the PG:Water binary mixture. To gain further insight of this initial observation, we have carried out the structural characterization of the PFL-PG-Water mixture, along with the microscopic dynamics water near propofol for the mentioned compositions (table 1).

Radial Distribution Function

The structure and dynamics of water around the drug-like molecules (propofol) play an important role in determining their solubility in the binary solution (PG:Water mixture). We have observed in the previous section that the propofol molecules in the lower propylene glycol content (S5) shows aggregation behavior, which is less probable in the higher propylene glycol content (S1). Such molecular level observation dictates the solubility of the drug-like molecules in the binary mixtures. So, it would therefore be interesting to examine the structure of water around the propofol (PFL) and propylene glycol (PG), and the structure of itself (PFL-PFL, PG-PG) with the variation of compositions. With this aim, we have estimated the radial distribution functions (equation.1) for OW(Water)−OW(Water), O1(PG)−OW(Water), O(PFL)−OW(Water), O1(PG)−O2(PG), and Center of Mass(PFL)-Center of Mass(PFL) atom pairs and plotted in figures 2a, 2b, 2c, 2d and 2e respectively.

$$g_{mn}(r) = \frac{V}{N^2}\langle \sum_{i}^{N_m} \sum_{j}^{N_n} \delta(r - r_{ij}) \rangle \tag{1}$$

The radial distribution function, g_{mn}(r), determine the distribution of a atom of type n from a reference atom of type m.[90]

In Fig. 2a, we have presented the radial distribution functions between oxygen atoms of water molecules, g_{OW-OW}(r), for five different compositions (table 1). The first peak is nearest around 0.28 nm, indicates the well defined first solvation shell around water oxygen (OW), followed by the unstructured second solvation shell, reported for TIP3P water model.[77] The intensity of the first peak and the first part up to 0.35 nm of the pair correlation functions truly depend on the propylene glycol content of PG:Water mixture. In g_{OW-OW}(r), the first peak intensity is an implication of more structured water network for higher propylene glycol content. Similar observation for solvent peak maxima enhancement with increase in solute concentration was reported in several other works.[91–93]

In Fig. 2b, we displayed the radial distribution function between the oxygen atom (O1) of the propylene glycol and water oxygen (OW) atom, $g_{O1PG-OW}$(r), for five different compositions (table 1). The major characteristic of $g_{O1PG-OW}$(r) for five different compositions, is a well defined first peak with altered intensity centered on 0.28 nm. Which indicates that the water corresponding to the first peak is more structured near O1PG for high propylene glycol content, and the change in intensity most probably the competitive nature of hydrophilic propylene glycol cluster formation by varying their composition in PG:Water mixture. In a report, Egorov et al. have observed the similar trends for other binary mixtures.[94]

The first peak of $g_{OPFL-OW}$(r) between the oxygen atom (O) of the propofol and water oxygen (OW) atom for five different compositions are shown in Fig. 2c, with the position of the peak are centered on 0.29 nm. The altered intensity of the first peak implies that the water in the first solvation of OPFL is more structured for higher propylene glycol vol/vol % ratio. The hydrophilic propylene glycol influences the stability of the water network as well as the stability of the micro-solvation shell around propofol, which may play a key role in the propofol dissolution process.

The distinctive features for oxygen(O1)−oxygen(O2) pair correlation function ($g_{O1PG-O2PG}(r)$) of propylene glycol hydroxyl oxygen atoms are observed in Fig. 2d for five compositions, with the position of the peak are centered on 0.3 nm. Followed by an interesting feature between 0.34 to 0.39 nm. In the pair correlation functions, the first peak corresponds to intra− and intermolecular O1−−O2 interactions, whereas the stepwise reduction of second peak intensity corresponds to intermolecular O1−−O2 interactions for five different PG:Water compositions. At low propylene glycol content (S5), the interaction between different PG hydroxyl oxygens is enhanced as observed in the peak intensity. The enhancement of peak intensity at low PG content (S5) suggests the significant self clustering of PG. On the other hand, In Fig. 2b we showed the $g_{O1PG-OW}(r)$ between propylene glycol oxygen (O1PG) and water oxygen (OW) atom, which indicates the propylene glycol prefers to be associated with water than to itself at higher propylene glycol content in PG:Water mixture.

In Fig. 2e, we displayed the pair correlation function ($g_{PFL-PFL}(r)$) between the center of mass of propofol molecules for the mentioned compositions (table 1). The $g_{PFL-PFL}(r)$, shows a broad complicated structure between 0.4 to 1.0 nm, and the contrasting intensities of the peak implies that the propofol molecules are forming aggregate for low propylene glycol content (S5), whereas the aggregation tendency becomes weaker for higher propylene glycol content in PG:Water mixture (S1). In Fig. 2b, the pair correlation function, $g_{O1PG-OW}(r)$, implies that the water is more structured for high propylene glycol content, and the similar trends of water network observed in $g_{OPFL-OW}(r)$ (Fig. 2c). Which implies the highly structured micro-solvation shell around propofol, may retard the aggregation process for larger propylene glycol content (S1). Conversely, the less ordering of the micro-solvation shell around propofol may facilitate the aggregation process for reduced propylene glycol content. Therefore, the micro-solvation shell around the propofol should be more structured for a successful dissolution process.

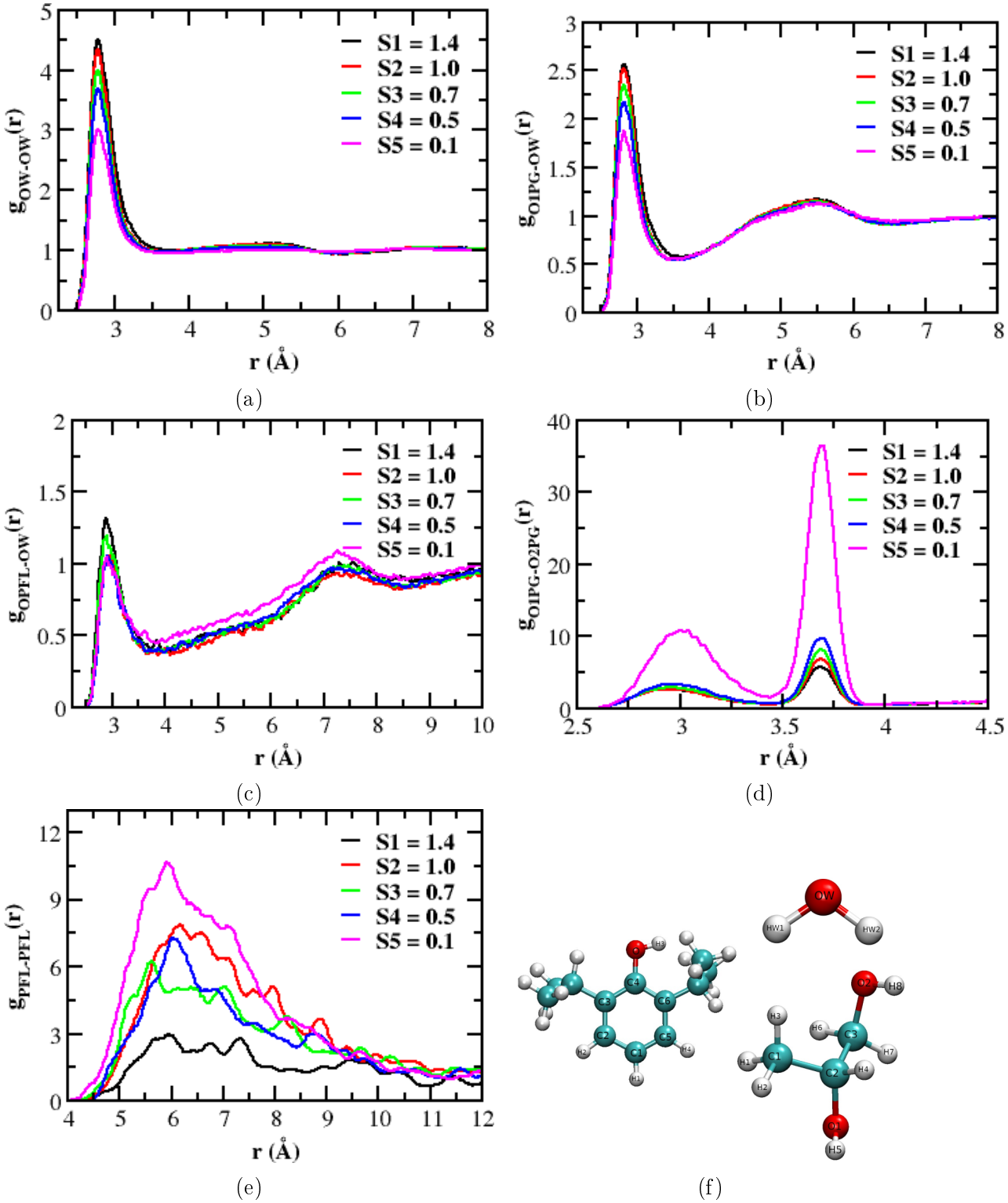

Figure 2: Radial distribution functions between (a) the oxygen atoms of water molecules, g_{OW-OW}(r), (b) the oxygen atom (O1) of the propylene glycol and water oxygen (OW) atom, $g_{O1PG-OW}$(r), (c) the oxygen atom (O) of the propofol and water oxygen (OW) atom, $g_{OPFL-OW}$(r), (d) the oxygen(O1)-oxygen(O2) of propylene glycol hydroxyl oxygen atoms, $g_{O1PG-O2PG}$(r), (e) the center of mass of propofol molecules, $g_{PFL-PFL}$(r) for five different compositions (table 1) of PG:Water mixture. (f) Ball and Stick representation of various constituents present in the proposed compositions (table 1), with atom labeling.

Water Microsolvation

The potentially different water around the propofol for various compositions, play a vital role in controlling their solubility in the PG:Water mixture. The differential nature of water micro-structure can influence both translational and reorientational dynamics of water next to the propofol, which is likely to control their solubility. In this section, we examine the dynamics of water near propofol for five different compositions.

Mean Square Displacements

The translational mobility of water molecules can be studied by monitoring the diffusion coefficient (D). Which can be obtained from the slope of the mean square displacement (MSD) vs time curve, using the well known Einstein relation.[95]

$$D = lim_{\delta t \to \infty} \frac{\left\langle |r(t) - r(0)|^2 \right\rangle}{2n\delta t} = lim_{\delta t \to \infty} \frac{\langle \Delta r^2 \rangle}{2n\delta t} \tag{2}$$

Where n is the dimensionality of the system, $r_i(0)$ and $r_i(t)$ are the coordinates of the ith water molecule oxygen atom at times t = 0 and t = t, respectively. The averaging $\langle .. \rangle$ is done over both time origins and water molecules.

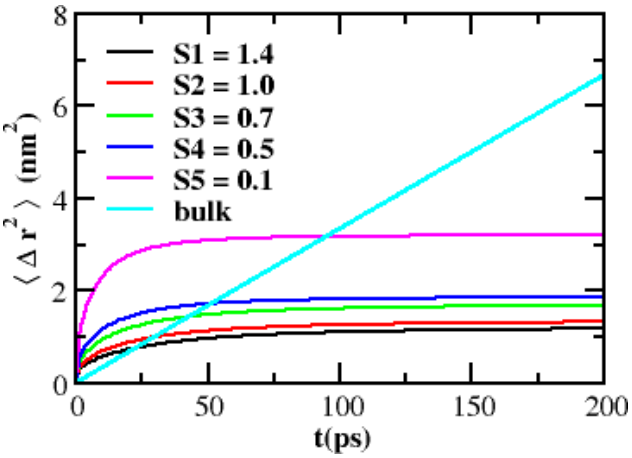

Figure 3: Mean square displacement (MSD) of the water molecules present in the micro-solvation shell of propofol. Water molecules that reside within 5 Åfrom the hydroxyl oxygen atom of the propofol are considered for calculation. For comparison, the MSD of the bulk water molecules is also incorporated.

We have calculated the mean square displacements of water molecules present in the micro-solvation shell around the propofol for five different compositions (table 1), which are displayed in Figure 3. In the calculations, we have considered only those water molecules, which reside within 5 Åfrom the hydroxyl oxygen atom of the propofol, defined as the micro-solvation shell. For comparison, we have incorporated the MSD for bulk water molecules, shows the water diffuse with a self-diffusion coefficient of $5.22\times\ 10^{-5}$ cm^2/s at 300 K. It is clear from the figure that the translational diffusion of water belongs to the micro-solvation shell of the propofol shows flat MSD curves for all five compositions, indicates the highly ordered water micro-structure network as compared to the bulk (Figure 2a). Such ordered phases exhibit damped diffusion, with minor displacement due to thermal agitation and orientational disordering caused by the presence of two isopropyl groups ortho to the hydroxyl group of propofol. Importantly, the MSD of water belongs to the micro-solvation shell of propofol for five different compositions is significantly different from one another, and the MSD curve of water for low propylene glycol content (S5) is higher as compared to the other

compositions, exhibiting the higher molecular libration against the equilibrium position of water that arrested with increasing the propylene glycol content in PG:Water mixture. However, the plateau in MSD reflects the availability of the space in the micro-solvation structure around propofol for low propylene glycol content is larger, and increasing the propylene glycol content the water micro-structure favors dense packing with lesser availability of space and restricted translation. Recently, Henao et al. have reported the similar diffusive behavior of water for various crystal phases.[96] Again, the water diffusion shows a variable dependence of the propylene glycol content in the PG:Water mixture, and the sluggish diffusion of water for high propylene glycol content due to the dominant role of propylene glycol-water interactions, favor the dense packing of water micro-structure around the propofol. In the recent past, Cerveny et. al. have observed the dielectric response of n-propylene glycol-water mixture, where restricted water mobility have been observed below critical water concentration.[50] They have shown that as the concentration of water molecules starts increasing more and more, the interactions within the water molecules increases as compared to n-propylene glycol-water interactions. Interestingly, there is a marked decrease in the mobility of water as the propylene glycol fraction in the solution increases. Similar observation of water diffusion with varied composition was reported by Luzar and Chandler[97] in their simulation study on dmso-water mixture.

The water mobility in the propofol micro-solvation shell for low propylene glycol content (S5) is higher as compared to the other compositions(table 1), whereas for higher propylene glycol content (S1) the water mobility is reduced. Such differential water mobility agrees well with the water micro-structure around propofol. Which indicates the higher ordering of water micro-solvation shell around propofol, as observed in the previous section for S1, depicts the restricted mobility of water in the propofol micro-solvation shell (Figure 3), results the hindered aggregation or favored dissolution process of propofol. However, the lower ordering of micro-solvation shell around propofol, as observed in the previous section

for S5, illustrate the un-restricted dynamics of water in the propofol micro-solvation shell (Figure 3), facilitates the aggregation process of propofol.

Reorientational Dynamics

In a varied composition of binary mixture containing drug-like molecules (propofol), the reorientational dynamics of water in the micro-solvation shell of the molecule can be influenced remarkably. Water molecule can switch its orientation by changing the hydrogen bond formed with the acceptor or donor molecule, and it's orientation often gets restricted in the presence of confinement, which can be geometric or electrostatic in nature, except for sub-ps libration motion which is possible due to the tumbling motion of broken hydrogen bond or any of free OH hand of water molecule. Therefore, rotation of water requires an exchange event and that can be hindered in the case where such exchange is less probable leading to retardation. The rotational motion of water can be monitored by calculating the reorientational dynamics of the OH vector of water. The time evolution of the OH vector of water can be monitored by calculating the orientational time correlation function. Which can be decayed to zero for orientationally disordered phases, but on the other hand, for orientationally ordered phases the orientations are correlated with one. The orientational time correlation function $C_l(t)$, is defined using the following equation :

$$C_l^{\mu}(t) = \left\langle P_l\left[\mu(0)\cdot\mu(t)\right]\right\rangle = \left\langle P_l\left[(cos\theta(t))\right]\right\rangle \tag{3}$$

where l is the order of legendre polynomial

$$P_1(x) = x \tag{4}$$

$$P_2(x) = (3x^2 - 1)/2 \tag{5}$$

and μ represents the vector of orientation in the molecule used for the calculation. The angular brackets indicating the averaging is over both the water molecules and time origins. Again, the calculated reorientation time can be correlated with experiments such as C_1(t) is observed in dielectric spectroscopy, and C_2(t) is observed in NMR and light scattering experiment.[95]

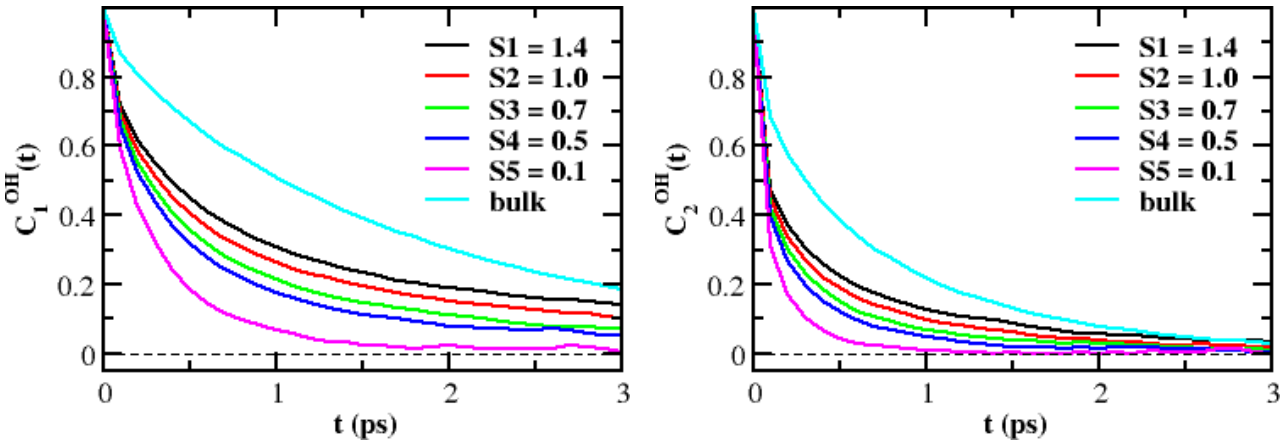

(a) (b)

Figure 4: Reorientational time correlation functions of the water OH vector, (a) $C_1{}^{OH}$(t) and (b) $C_2{}^{OH}$(t), for the water present in the micro-solvation shell around the propofol for five different compositions. The relaxation for bulk water molecules is incorporated for comparison.

To investigate the effect on rotational behavior of water present in the micro-solvation shell around the propofol for all five compositions, the first and second order Legendre orientational correlation function (OCF) of OH vector of water has been calculated and presented in fig 4. For comparison, we have also introduced the correlation function for bulk water molecules. It is evident from the figure that the water reorientation becomes slower as the PG:Water mixture composition tending towards high propylene glycol content. However, the OCF relaxation of micro-solvation shell water for all five compositions is faster as compared to the bulk water. Which can be interpreted from the fact that the bulk water has orientational and translational motions coupled. Such molecular coupling becomes weaker

for water belonging to micro-solvation shells. Since, they usually utilize their energy for molecular rotation, and very minimal for translation. The rotational behavior of water follows a monotonic composition dependence, suggests the faster OCF decay of water correspondence to the unstable water micro-solvation shell near the propofol for low propylene glycol content (S5), as discussed in the earlier section. Such unstable water micro-solvation shells near the propofol favored their aggregation behavior. The damped reorientation of water in the propofol micro-solvation shell for large propylene glycol content (S1), signifies the stable water micro-network around the propofol, which truly depends on the propylene glycol−water interactions, discussed earlier. In the higher concentration of propylene glycol, forms small pockets of water network where propofol resides and be solvated in those pockets, and expedite the dissolution process.

The OCFs shown in Figure 4, can be expressed as an exponential function $e^{-t/\tau}$, and the ratio between the first and second order reorientation times (τ_1/τ_2) provides information about the kind the orientation. The more diffusive molecular rotation consist of small amplitude angular jumps,[98] and the OCF decay can be expressed exponentially with the following equation:

$$C_l^{OH}(t) = e^{-l(l+1)D_{rot}t} \tag{6}$$

and the relaxation time as:

$$\tau_l^{-1} = l(l+1)D_{rot} \tag{7}$$

with ratio $\tau_1/\tau_2 = 3$, and verifying this value signify the rigorous test for the Debye model. The rotations consistent with small angular jumps corresponds to higher τ_1/τ_2 values, and the large angular jumps corresponds to the smaller τ_1/τ_2 values.

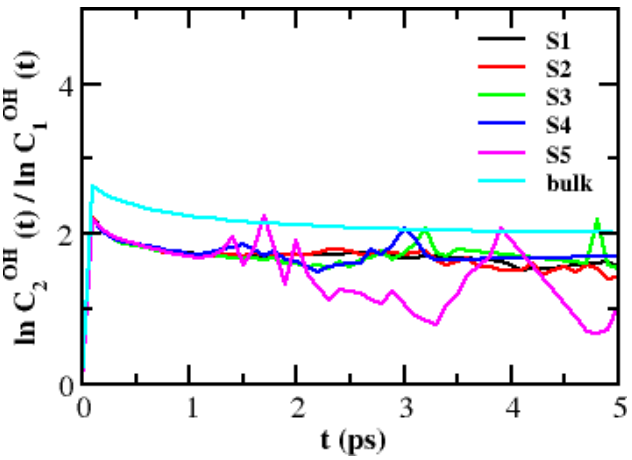

Figure 5: The ratio of first and second order reorientation times ($\ln(C_2^{OH}(t))/\ln(C_1^{OH}(t))$) of the OH vector for the water molecules belongs to the micro-solvation shell around the propofol for five different compositions. The ratio for bulk water molecules is incorporated for comparison.

In Figure 5, we displayed the ratio of τ_1/τ_2, for bulk water the value is closer to 2 in the long time limit, and for propofol micro-solvation shell water the value deviating slightly from 2. Which indicates that the reorientation in the water micro-solvation shells take place for large-amplitude angular jumps, as observed in the bulk water.[99] The smaller values of the ratio for water are monitored previously.[100–102] Importantly, the deviation of ratio τ_1/τ_2 from the bulk value ($\tau_1/\tau_2 \approx 2$) for propofol micro-solvation shells may alter the hydrogen bond lifetime, and in the next sub-section the hydrogen bond dynamics between propofol and water molecules belongs to the micro-solvation shells and its conceptual implications for propofol dissolution process will be discussed.

Hydrogen Bond Dynamics

The water micro-structural network and the dynamics of water molecules present in the propofol micro-solvation shell are influenced by the isopropyl groups ortho to sterically hindered hydroxyl group, and the steric hindrance by two alkyl groups hindered the formation

of hydrogen bond in aqueous medium. So, the hydrogen bond dynamics play a vital role in determining the solubility of propofol molecules in PG:Water mixtures. The hydrogen bond can be defined as either a geometric[103–105] or an energetic[106] criteria. However, we have opted for a geometric criteria to define a hydrogen bond.[103–105]

To observed the structural relaxation of hydrogen bonds, one can use the time correlation function, defined as[107]

$$C_{HB}(t) = \big\langle h(t+\tau)h(\tau)\big\rangle / \big\langle h(\tau)h(\tau)\big\rangle \tag{8}$$

Where the dynamical variable h(t) is equal to unity for a specific pair of propofol−−water or water−−water sites is hydrogen bonded at time t, and is zero otherwise. In this work, we have opted purely geometric criteria to define a hydrogen bond, the propofol-water pair is considered to be hydrogen bonded, if the O(PFL)− − −OW and O(PFL)− − −HW1/HW2 distances are smaller than 0.35 nm and 0.25 nm, respectively, and the O(PFL)− − −OW− − −HW1/HW2 angle is smaller than 30 °, and the water-water pair is treated to be hydrogen bonded, if the OW− − −OW distance is smaller than 0.35 nm and the OW− − −OW− − −HW1/HW2 angle is smaller than 30 °.[104,105] The angular brackets indicate averaging over all pair of hydrogen bonds and over τ (initial times). The C_{HB}(t) designates the probability that the hydrogen bond between the specific propofol−−water or water−−water pair is intact at time t+τ (h(t+τ)=1), given it was intact at time τ (h(τ)=1). So, the C_{HB}(t) allows re-formation of the broken bond, which loose the hydrogen bond criteria at some intermediate time. Thus, it allows recrossing the bonded and nonbonded states energy barrier. It also measures the correlation of hydrogen bonds independent of possible bond breaking events, and commonly termed as "intermittent hydrogen bond correlation function".[107,108] Importantly, the C_{HB}(t) relaxation gives the information about the structural relaxation of a hydrogen bond pair.

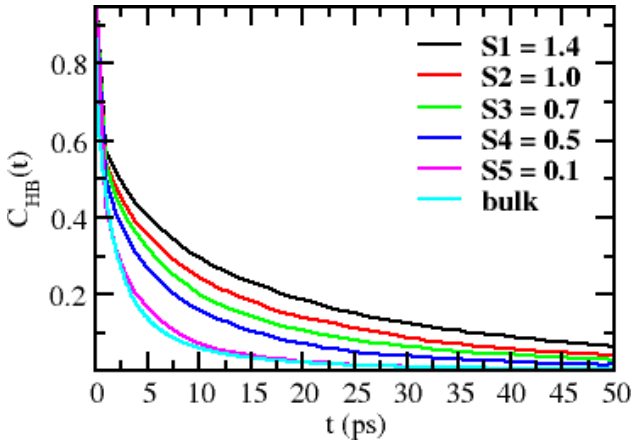

Figure 6: Intermittent Hydrogen bond time correlation function, $C_{HB}(t)$, for the hydrogen bonds formed between the propofol and the water molecules present in the micro-solvation shell around the propofol for all five compositions. The same for the water-water hydrogen bond for bulk water molecules is incorporated for comparison.

In Figure 6, we showed the time correlation function for the hydrogen bond formed between the propofol and the water molecules present in the micro-solvation shell around the propofol for five different compositions (table 1). The same for the hydrogen bond formed between a pair of bulk water molecules is included for comparison. The $C_{HB}(t)$ for bulk water has been estimated from a molecular dynamics (MD) simulation of TIP3P water under similar thermodynamic conditions. It is noticed from the figure that the structural relaxation of propofol−−water hydrogen bond is slower as compared to the bulk water counterpart. Interestingly, the figure exhibit the propofol−−water hydrogen bond relaxation for all five compositions is notably different from one another, and the relaxation for higher propylene glycol content (S1) is slower as compared to the rest. The relaxation pattern clearly indicates the existence of slow components for all five compositions, which can be described by multi-exponential law.[103] The Figure 6 resemble the contrasting rigidity of the micro-solvation shells around propofol for five different compositions. Further, the structural relaxation of the hydrogen bonds formed between propofol and water belongs to micro-solvation shells shows a variable dependence of the propylene glycol content in the PG:Water mixture, and

the slower relaxation of propofol−−water hydrogen bonds for high propylene glycol content (S1) because of the major role played by propylene glycol− − − water interactions. Which influence the formation of ordered water micro-structure network around propofol for S1, S2 and restrict the mobility of water in the micro-solvation shells. Again, the relaxation behavior towards low propylene glycol content is faster in respect of the other compositions (table 1). Such a key observation agrees nicely with the decreasing trends of ordering of water micro-solvation shell around propofol for lowering the propylene glycol content in the PG:Water mixture, which is in accordance with faster reorientation of the micro-solvation shell water for S4 and S5, observed previous section, favoring the aggregation process of propofol at low propylene glycol content.

Residence Time

The residence time provides information about the dynamical nature of the water micro-structure around propofol. The differential behavior of water micro-structure around propofol due to varying interactions of water with propylene glycol in different compositions of PG:Water mixture. Thus, the altering propylene glycol− − −water interactions can give rise to unusual structural relaxation of water micro-solvation shell around propofol for five different compositions. To characterize the structural relaxation of the micro-solvation shell around the propofol molecule, we have constructed the intermittent residence time correlation function, R(t), which describes the probability that a particular molecule stays in a given region at time t, given it existed at the initial time. We defined the intermittent residence time correlation function as,

$$R_j(t) = \frac{\langle \theta_j(\tau)\theta_j(t+\tau)\rangle}{\langle \theta_j(\tau)\theta_j(\tau)\rangle} \tag{9}$$

where the population variable $\theta_j(t)$ is unity when the molecule r_i is present in a given

region j at time t, and zero otherwise. So, during simulation individual molecules can exit and enter in the different regions, and the above correlation function is developed based on the residence time of all molecules present in the region j. The angular brackets denote averaging over all molecules present in the particular region, and over initial times τ. The correlation function $R_j(t)$ describes the probability that a particular molecule stays in a given region j at time t+τ ($\theta_j(t+\tau)$=1), given it was exist at time τ ($\theta_j(\tau)$=1). So, the $R_j(t)$ allows the re-visit of the molecule that exits at the intermediate time from region j. Thus the intermittent residence time correlation function, $R_j(t)$, estimates the correlation of molecular residence at the region j is independent of possible entry-exit events in the particular region. Therefore, the relaxation of $R_j(t)$ furnishes the information about the structural mobility of a specific region.

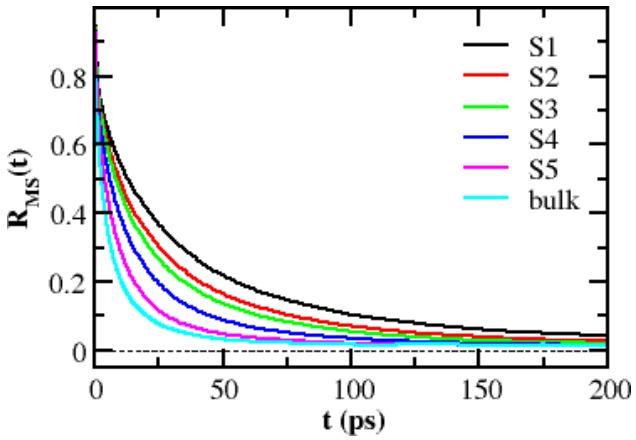

Figure 7: Intermittent residence time correlation function, $R_{MS}(t)$, for the water molecules present in the micro-solvation shell around the propofol for five different compositions (table 1). The same for bulk water molecules is incorporated for comparison.

We have measured the intermittent residence time correlation function, $R_{MS}(t)$, for the water molecules belongs to the micro-solvation shell around the propofol for all five compositions, and displayed in Figure 7. In the calculations, we have opted only for those water molecules present within 5 Åfrom the hydroxyl oxygen atom of the propofol, defined as the

region for residence time estimation (j). For comparison, we have incorporated the same for bulk water molecules. It is clear from the figure that the relaxation for all five compositions shows a faster short time decay followed up with a long time tail. The initial rapid relaxation due to the molecular libration, which moves the boundary molecules out of the defined region because of short displacements. However, the origin of the long time decay comes from the structural relaxation of the micro-solvation shell around the propofol. So, the observed relaxation of $R_{MS}(t)$ cannot be modeled by a single-exponential law. The sum of three exponentials (Equation 10) have been used to model the distribution of residence times as well as the long time decay. The parameters for best fit are displayed in Table 2.

$$R_{MS}(t) = a1 * e^{-(t/\tau_1)} + a2 * e^{-(t/\tau_2)} + a3 * e^{-(t/\tau_3)} \tag{10}$$

$$\langle \tau_{residence} \rangle = \frac{\sum_{i=1}^{3} a_i \tau_i}{\sum_{i=1}^{3} a_i} \tag{11}$$

Table 2: Multiexponential Fitting Parameters for the Intermittent Residence Time Correlation Function of Water Molecules belongs to the Micro-solvation Shell of Propofol

System	a1	τ_1 (ps)	a2	τ_2 (ps)	a3	τ_3 (ps)	$\langle \tau_{residence} \rangle$ (ps)
S1	0.26	0.87	0.53	25.88	0.21	127.72	40.76
S2	0.28	0.98	0.56	22.10	0.16	114.68	31.00
S3	0.28	0.96	0.57	19.31	0.15	101.57	26.51
S4	0.30	0.89	0.60	15.56	0.10	103.37	19.94
S5	0.34	0.99	0.61	11.69	0.05	137.74	14.36
Bulk Water	0.20	0.25	0.50	3.77	0.30	18.38	7.45

It appears in the multi-exponential fit that the $\langle \tau_{residence} \rangle$ value of the water micro-solvation shell around propofol for all five compositions is higher than the bulk water. Again, the relaxation of $R_{MS}(t)$ for the water micro-solvation shell around the propofol for all five compositions is remarkably different from one another, and it is observed the existence of

short and long time components. As mentioned above, the presence of the long time decay due to the structural relaxation of the water micro-structure present around the propofol. Further, we need to explore this aspect more microscopically. The multi-exponential fit, Table 2, displayed the average intermittent residence time relaxation ($\langle\tau_{residence}\rangle$) for water belongs to micro-solvation shell around propofol for S1 is approximately three times higher in comparison to S5. Such remarkably slower relaxation due to the substantial contribution of the long time component of about (a3*τ_3 = 26.82 ps) for micro-solvation water around S1, which is larger than that of the other four compositions (18.35 ps(S2), 15.24 ps(S3), 10.34 ps(S4), 6.89 ps(S5)). So, the high propylene glycol content (S1) shows the slower structural relaxation of the micro-solvation shell around propofol, which turns into faster relaxation as the propylene glycol content approaches low concentration. However, the $R_{MS}(t)$ relaxation depicts a dependence on propylene glycol content in the PG:Water mixture, supporting the dominant role of the propylene glycol$---$water interactions in controlling the structural relaxation of the micro-solvation shell. Which designates the slower structural relaxation of micro-solvation shells around propofol, corresponds to the higher ordering of water micro-structure and restricted water mobility, results in the favorable dissolution process of propofol at higher propylene glycol content in PG:Water mixture. On the other hand, the faster structural relaxation of water micro-solvation shell around propofol, supports the lower ordering of water micro-structure and un-restricted water dynamics in the micro-solvation shell, prefer the aggregation process at low propylene glycol content in the PG:Water mixture.

Conclusions

In this paper, we have studied in detail the structure and dynamics of water present in the micro-solvation shells around propofol for five different compositions (table 1). The simulation studies revealed that the propofol in the propylene glycol : water mixture mod-

ulates their internal structure formation, resulting in clustering with varying composition of propylene glycol content during the nanosecond timescale of the simulation. We monitored that the propylene glycol tends to interact more with itself than with water at the low molecular (propylene glycol) ration in the PG:Water mixture. Although, the pair correlation function depicts a more ordered water micro-structure around propofol for high propylene glycol content in the PG:Water mixture. Hence, the hydrophilic propylene glycol controls the stability of the water network in the mixture, resulting in the ordered structure of the water micro-solvation shell around propofol that plays a crucial role in the PFL dissolution process. We noticed the translational and rotational behavior of water belonging to the propofol micro-solvation shell is restricted for high propylene glycol content (S1), whereas the water mobility is relaxed towards the low propylene glycol content in the PG:Water mixture. The structural relaxation of the hydrogen bond formed between the propofol and the water molecules present in the micro-solvation shell around the propofol for five different compositions, is found slower as compared to the bulk water, and distinct from one another. We also observed that the structural relaxation of the mentioned hydrogen bond for higher propylene glycol content (S1) is slower as compared to the others, which tends to be faster in the direction of low propylene glycol content. So, the propofol−−water hydrogen bond relaxation resembles the contrasting rigidity of the micro-solvation shells around propofol for all five compositions. However, the intermittent residence time correlation function for the water molecules belonging to the micro-solvation shell around the propofol for five different compositions displayed a faster short time decay followed up with a long time tail. The initial rapid relaxation corresponds to the molecular libration, and the origin of the long time decay from the structural relaxation of the micro-solvation shell around the propofol. Interestingly, the relaxation of water micro-solvation shells around the propofol for all five compositions is distinguishable from one another, and the high propylene glycol content shows the slower structural relaxation that turns faster as the propylene glycol content approaches low value.

The relaxation behavior depicts a dependence on propylene glycol content in the binary mixture, which supports the dominant role of the propylene glycol−−water interactions in controlling the structural relaxation of the micro-solvation shell. Although, this aspects require further verification, and under major examination in our laboratory. So, our observations designate that the slower structural relaxation of the micro-solvation shell around propofol, corresponds to the extensive ordering of water micro-structure and restricted water mobility, results in the favorable dissolution process of propofol at higher propylene glycol content in PG:Water mixture. However, the faster structural relaxation of the similar water environment, supports the insignificant ordering of water micro-structure and un-restricted water dynamics, facilitates the aggregation process of propofol at low propylene glycol content in the PG:Water mixture.

Data and Software Availability

The parallel MD simulation package GROMACS-2018.3 has been used to conduct all the simulation. The software can be found at https://manual.gromacs.org/2018.3/index.html. The CHARMM General Force Field (CGenFF) used to obtained the propylene glycol parameters, and the CHARMM modified TIP3P water model used to model the solvent and may be found at https://www.charmm.org/archive/charmm/resources/charmm-force-fields/ . We used the VMD-1.9.3 graphics software to build molecular structure and snapshots. The graphics software may be found at https://www.ks.uiuc.edu/Research/vmd/ . We have used several in-house codes to obtained the results reported in this article. The in-house analysis codes and the allied input files can be accessed from https://github.com/anupama-creator/correlations_calc.

Acknowledgements

This work was supported in part by generous grants from the University Grants Commission (UGC)-BSR Start-up grant (F.30-432/2018(BSR)), Central University of Punjab - Research Seed Money, Department of Science and Technology (DST) under Fast Track Scheme for Young Scientist (SB/FT/CS-158/2013), Government of India. A.S. thanks CSIR for providing a scholarship. S.C. is thankful to Prof. Raghavendra P. Tiwari, Vice Chancellor, Central University of Punjab Bathinda, for encouraging the research and providing the necessary facilities.

References

(1) Fasinu, P.; Pillay, V.; Ndesendo, V. M.; du Toit, L. C.; Choonara, Y. E. Diverse approaches for the enhancement of oral drug bioavailability. *Biopharmaceutics & drug disposition* **2011**, *32*, 185–209.

(2) Das, T.; Mehta, C. H.; Nayak, U. Y. Multiple approaches for achieving drug solubility: an in silico perspective. *Drug discovery today* **2020**, *25*, 1206–1212.

(3) Chaban, V. V.; Savchenko, T. I.; Kovalenko, S. M.; Prezhdo, O. V. Heat-driven release of a drug molecule from carbon nanotubes: a molecular dynamics study. *The Journal of Physical Chemistry B* **2010**, *114*, 13481–13486.

(4) Smith, D. J.; Shah, J. K.; Maginn, E. J. Molecular dynamics simulation study of the association of lidocainium docusate and its derivatives in aqueous solution. *Molecular Pharmaceutics* **2015**, *12*, 1893–1901.

(5) Riveros-Perez, E.; Riveros, R. Water in the human body: An anesthesiologist's per-

spective on the connection between physicochemical properties of water and physiologic relevance. *Annals of medicine and surgery* **2018**, *26*, 1–8.

(6) Nury, H.; Van Renterghem, C.; Weng, Y.; Tran, A.; Baaden, M.; Dufresne, V.; Changeux, J.-P.; Sonner, J. M.; Delarue, M.; Corringer, P.-J. X-ray structures of general anaesthetics bound to a pentameric ligand-gated ion channel. *Nature* **2011**, *469*, 428–431.

(7) Willenbring, D.; Xu, Y.; Tang, P. The role of structured water in mediating general anesthetic action on $\alpha 4\beta 2$ nAChR. *Physical Chemistry Chemical Physics* **2010**, *12*, 10263–10269.

(8) Li, C.; Xu, Q.; Chen, X.; Li, R. Bezafibrate in several aqueous mixtures of low alcohols: solubility, solvent effect and preferential solvation. *The Journal of Chemical Thermodynamics* **2021**, *156*, 106208.

(9) Baksi, A.; Biswas, R. Does Confinement Modify Preferential Solvation and H-Bond Fluctuation Dynamics? A Molecular Level Investigation through Simulations of a Bulk and Confined Three-Component Mixture. *The Journal of Physical Chemistry B* **2020**, *124*, 11718–11729.

(10) Sridhar, A.; Johnston, A. J.; Varathan, L.; McLain, S. E.; Biggin, P. C. The solvation structure of alprazolam. *Physical Chemistry Chemical Physics* **2016**, *18*, 22416–22425.

(11) Aydi, A.; Ortiz, C. P.; Caviedes-Rubio, D. I.; Ayadi, C.; Hbaieb, S.; Delgado, D. R. Solution thermodynamics and preferential solvation of sulfamethazine in ethylene glycol+ water mixtures. *Journal of the Taiwan Institute of Chemical Engineers* **2021**, *118*, 68–77.

(12) Holguin, A. R.; Delgado, D. R.; Martinez, F.; Marcus, Y. Solution thermodynamics

and preferential solvation of meloxicam in propylene glycol+ water mixtures. *Journal of solution chemistry* **2011**, *40*, 1987–1999.

(13) Dasari, S.; Mallik, B. S. Solubility and solvation free energy of a cardiovascular drug, LASSBio-294, in ionic liquids: A computational study. *Journal of Molecular Liquids* **2020**, *301*, 112449.

(14) Huang, Y.; Ji, Y.; Zhang, M.; Ouyang, D. How imidazolium-based ionic liquids solubilize the poorly soluble ibuprofen? A theoretical study. *AIChE Journal* **2020**, *66*, e16940.

(15) Kaiser, A.; Ritter, M.; Nazmutdinov, R.; Probst, M. Hydrogen bonding and dielectric spectra of ethylene glycol–water mixtures from molecular dynamics simulations. *The Journal of Physical Chemistry B* **2016**, *120*, 10515–10523.

(16) Gubskaya, A.; Kusalik, P. Molecular dynamics simulation study of ethylene glycol, ethylenediamine, and 2-aminoethanol. 2. Structure in aqueous solutions. *The Journal of Physical Chemistry A* **2004**, *108*, 7165–7178.

(17) Roy, S.; Bagchi, B. Solvation dynamics of tryptophan in water-dimethyl sulfoxide binary mixture: In search of molecular origin of composition dependent multiple anomalies. *The Journal of chemical physics* **2013**, *139*, 034308.

(18) Zhang, X.; Wang, Z.; Chen, Z.; Li, H.; Zhang, L.; Ye, J.; Zhang, Q.; Zhuang, W. Molecular Mechanism of Water Reorientation Dynamics in Dimethyl Sulfoxide Aqueous Mixtures. *The Journal of Physical Chemistry B* **2020**, *124*, 1806–1816.

(19) Walsh, C. T. Propofol: milk of amnesia. *Cell* **2018**, *175*, 10–13.

(20) Adler, A. C. Propofol: review of potential risks during administration. *AANA journal* **2017**, *85*, 104.

(21) Garcia, P. S.; Kolesky, S. E.; Jenkins, A. General anesthetic actions on GABAA receptors. *Current neuropharmacology* **2010**, *8*, 2.

(22) Oakes, V.; Domene, C. Capturing the molecular mechanism of anesthetic action by simulation methods. *Chemical reviews* **2018**, *119*, 5998–6014.

(23) Dutta, M.; Gilbert, S. P.; Onuchic, J. N.; Jana, B. Mechanistic basis of propofol-induced disruption of kinesin processivity. *Proceedings of the National Academy of Sciences* **2021**, *118*, e2023659118.

(24) Wang, Y.; Yang, E.; Wells, M. M.; Bondarenko, V.; Woll, K.; Carnevale, V.; Granata, D.; Klein, M. L.; Eckenhoff, R. G.; Dailey, W. P., et al. Propofol inhibits the voltage-gated sodium channel NaChBac at multiple sites. *Journal of General Physiology* **2018**, *150*, 1317–1331.

(25) Lemaitre, F.; Hasni, N.; Leprince, P.; Corvol, E.; Belhabib, G.; Fillâtre, P.; Luyt, C.-E.; Leven, C.; Farinotti, R.; Fernandez, C., et al. Propofol, midazolam, vancomycin and cyclosporine therapeutic drug monitoring in extracorporeal membrane oxygenation circuits primed with whole human blood. *Critical Care* **2015**, *19*, 1–6.

(26) Thompson, K. A.; Goodale, D. B. The Recent Development of Propofol (DIPRIVAN^ sup®^). *Intensive care medicine* **2000**, *26*, S400.

(27) McCulloch, M.; Lees, N. Assessment and modification of pain on induction with propofol (Diprivan). *Anaesthesia* **1985**, *40*, 1117–1120.

(28) Eriksson, M.; Englesson, S.; Niklasson, F.; Hartvig, P. Effect of lignocaine and pH on propofol-induced pain. *British journal of anaesthesia* **1997**, *78*, 502–506.

(29) Wolf, A.; Weir, P.; Segar, P.; Stone, J.; Shield, J. Impaired fatty acid oxidation in propofol infusion syndrome. *The Lancet* **2001**, *357*, 606–607.

(30) White, P. F. Propofol formulation and pain on injection. *Anesthesia & Analgesia* **2002**, *94*, 1042.

(31) Rieschke, P.; LaFleur, B. J.; Janicki, P. K. Effects of EDTA-and sulfite-containing formulations of propofol on respiratory system resistance after tracheal intubation in smokers. *The Journal of the American Society of Anesthesiologists* **2003**, *98*, 323–328.

(32) King, C. A.; Ogg, M. Safe injection practices for administration of propofol. *AORN journal* **2012**, *95*, 365–372.

(33) Baker, M. T.; Naguib, M.; Warltier, D. C. Propofol: the challenges of formulation. *The Journal of the American Society of Anesthesiologists* **2005**, *103*, 860–876.

(34) Damitz, R.; Chauhan, A.; Gravenstein, N. Propofol emulsion-free drug concentration is similar between batches and stable over time. *Romanian Journal of Anaesthesia and Intensive Care* **2016**, *23*, 7.

(35) Trapani, A.; Laquintana, V.; Lopedota, A.; Franco, M.; Latrofa, A.; Talani, G.; Sanna, E.; Trapani, G.; Liso, G. Evaluation of new propofol aqueous solutions for intravenous anesthesia. *International journal of pharmaceutics* **2004**, *278*, 91–98.

(36) Shityakov, S.; Salmas, R. E.; Durdagi, S.; Salvador, E.; Papai, K.; Yanez-Gascon, M. J.; Perez-Sanchez, H.; Puskas, I.; Roewer, N.; Forster, C.; Broscheit, J. A. Characterization, in vivo evaluation, and molecular modeling of different propofol–cyclodextrin complexes to assess their drug delivery potential at the blood–brain barrier level. *Journal of chemical information and modeling* **2016**, *56*, 1914–1922.

(37) Satti, J. R.; Das, D. K.; Ray, D. Investigation of the thermal conductivity of propylene glycol nanofluids and comparison with correlations. *International Journal of Heat and Mass Transfer* **2017**, *107*, 871–881.

(38) Liu, J.-H.; Gao, D.; He, L.-Q.; Moey, L. K.; Hua, K.; Liu, Z.-B. The phase diagram for the ternary system propylene glycol-sodium chloride-water and their application to platelet cryopreservation. *Zhongguo shi yan xue ye xue za zhi* **2003**, *11*, 92–95.

(39) Malajczuk, C. J.; Hughes, Z. E.; Mancera, R. L. Molecular dynamics simulations of the interactions of DMSO, mono-and polyhydroxylated cryosolvents with a hydrated phospholipid bilayer. *Biochimica et Biophysica Acta (BBA)-Biomembranes* **2013**, *1828*, 2041–2055.

(40) Hughes, Z. E.; Malajczuk, C. J.; Mancera, R. L. The effects of cryosolvents on DOPC-β-sitosterol bilayers determined from molecular dynamics simulations. *The Journal of Physical Chemistry B* **2013**, *117*, 3362–3375.

(41) Watkinson, R.; Guy, R.; Hadgraft, J.; Lane, M. Optimisation of cosolvent concentration for topical drug delivery–II: influence of propylene glycol on ibuprofen permeation. *Skin pharmacology and physiology* **2009**, *22*, 225–230.

(42) Yamane, M.; Williams, A.; Barry, B. Terpene penetration enhancers in propylene glycol/water co-solvent systems: effectiveness and mechanism of action. *Journal of pharmacy and pharmacology* **1995**, *47*, 978–989.

(43) Elsayed, M. M.; Abdallah, O. Y.; Naggar, V. F.; Khalafallah, N. M. PG-liposomes: novel lipid vesicles for skin delivery of drugs. *Journal of Pharmacy and Pharmacology* **2007**, *59*, 1447–1450.

(44) Aye, M.; Di Giorgio, C.; De Mo, M.; Botta, A.; Perrin, J.; Courbiere, B. Assessment of the genotoxicity of three cryoprotectants used for human oocyte vitrification: dimethyl sulfoxide, ethylene glycol and propylene glycol. *Food and chemical toxicology* **2010**, *48*, 1905–1912.

(45) Andersen, F. Final report on the safety assessment of propylene-glycol and polypropylene glycols. *Journal of the American College of Toxicology* **1994**, *13*, 437–491.

(46) Center for the Evaluation of Risks to Human Reproduction. NTP-CERHR Expert panel report on the reproductive and developmental toxicity of propylene glycol. *Reproductive Toxicology* **2004**, *18*, 533–579.

(47) Sjostrom, J.; Mattsson, J.; Bergman, R.; Swenson, J. Hydrogen bond induced non-monotonic composition behavior of the glass transition in aqueous binary mixtures. *The Journal of Physical Chemistry B* **2011**, *115*, 10013–10017.

(48) Bednarska, D.; Koniorczyk, M. The influence of diol addition on water crystallization kinetics in mesopores. *Journal of Thermal Analysis and Calorimetry* **2019**, *138*, 2323–2337.

(49) Elamin, K.; Björklund, J.; Nyhlén, F.; Yttergren, M.; Mårtensson, L.; Swenson, J. Glass transition and relaxation dynamics of propylene glycol–water solutions confined in clay. *The Journal of chemical physics* **2014**, *141*, 034505.

(50) Cerveny, S.; Schwartz, G.; Alegria, A.; Bergman, R.; Swenson, J. Water dynamics in n-propylene glycol aqueous solutions. *The Journal of chemical physics* **2006**, *124*, 194501.

(51) Kearney, M.-C.; McKenna, P. E.; Quinn, H. L.; Courtenay, A. J.; Larrañeta, E.; Donnelly, R. F. Design and development of liquid drug reservoirs for microneedle delivery of poorly soluble drug molecules. *Pharmaceutics* **2019**, *11*, 605.

(52) Delgado, D. R.; Romdhani, A.; Martínez, F. Solubility of sulfamethizole in some propylene glycol+ water mixtures at several temperatures. *Fluid phase equilibria* **2012**, *322*, 113–119.

(53) Vahdati, S.; Shayanfar, A.; Hanaee, J.; Martínez, F.; Acree Jr, W. E.; Jouyban, A. Solubility of carvedilol in ethanol+ propylene glycol mixtures at various temperatures. *Industrial & Engineering Chemistry Research* **2013**, *52*, 16630–16636.

(54) Jiménez, D. M.; Cárdenas, Z. J.; Martínez, F. Solubility and apparent specific volume of some pharmaceutical salts in propylene glycol+ water mixtures at 298.15 K. *Chemical Engineering Communications* **2016**, *203*, 1013–1019.

(55) Gao, Y.; Olsen, K. W. Molecular dynamics of drug crystal dissolution: simulation of acetaminophen form I in water. *Molecular pharmaceutics* **2013**, *10*, 905–917.

(56) Dwyer, C.; Viebke, C.; Meadows, J. Propofol induced micelle formation in aqueous block copolymer solutions. *Colloids and Surfaces A: Physicochemical and Engineering Aspects* **2005**, *254*, 23–30.

(57) Cho, J.; Cho, J. C.; Lee, P.; Lee, M.; Oh, E. Formulation and evaluation of an alternative triglyceride-free propofol microemulsion. *Archives of pharmacal research* **2010**, *33*, 1375–1387.

(58) Momot, K. I.; Kuchel, P. W.; Chapman, B. E.; Deo, P.; Whittaker, D. NMR study of the association of propofol with nonionic surfactants. *Langmuir* **2003**, *19*, 2088–2095.

(59) Biswas, B.; Singh, P. C. The enhanced dissociation and associated surface structure of the anesthetic propofol at the water interface: vibrational sum frequency generation study. *Physical Chemistry Chemical Physics* **2021**, *23*, 24646–24651.

(60) Tams, C.; Johnson, K. Prediction variability of combined pharmacokinetic pharmacodynamic models: a simulation study of propofol in combination with remifentanil and fentanyl. *J Anesth Clin Res* **2014**, *5*, 2.

(61) León, I.; Millán, J.; Castaño, F.; Fernández, J. A. A spectroscopic and computational study of propofol dimers and their hydrated clusters. *ChemPhysChem* **2012**, *13*, 3819–3826.

(62) Wang, H. J.; Kleinhammes, A.; Tang, P.; Xu, ., Y; Wu, Y. Critical role of water in the binding of volatile anesthetics to proteins. *J. Phys. Chem. B* **2013**, *117*, 12007–12012.

(63) LeBard, D. N.; Henin, J.; Eckenhoff, R. G.; Klein, M. L.; Brannigan, G. General Anesthetics Predicted to Block the GLIC Pore with Micromolar Affinity. *PLoS Comput Biol* **2012**, *8*, e1002532–1–9.

(64) Henin, J.; Brannigan, G.; Dailey, W. P.; Eckenhoff, R.; Klein, M. L. An atomistic model for simulations of the general anesthetic isoflurane. *J. Phys. Chem. B.* **2010**, *114*, 604–612.

(65) Liu, D. X. Y., L. T.; Willenbring; Tang, P. General anesthetic binding to neuronal $\alpha_4\beta_2$ nicotinic acetylcholine receptor and its effect on global dynamics. *J. Phys. Chem. B.* **2009**, *113*, 12581–9.

(66) Arcario, M. J.; Mayne, C. G.; Tajkhorshid, E. Atomistic models of general anesthetics for use in in silico biological studies. *The Journal of Physical Chemistry B* **2014**, *118*, 12075–12086.

(67) Koubi, L.; Tarek, M.; Bandyopadhyay, S.; L.;, K. M.; Scharf, D. Membrane structural perturbations caused by anesthetics and nonimmobilizers: A molecular dynamics investigation. *Biophys. J.* **2001**, *81*, 3339–3345.

(68) Faulkner, C.; Santos-Carballal, D.; Plant, D. F.; de Leeuw, N. H. Atomistic molecular dynamics simulations of propofol and fentanyl in phosphatidylcholine lipid bilayers. *ACS omega* **2020**, *5*, 14340–14353.

(69) Hansen, A. H.; Sørensen, K. T.; Mathieu, R.; Serer, A.; Duelund, L.; Khandelia, H.; Hansen, P. L.; Simonsen, A. C. Propofol modulates the lipid phase transition and localizes near the headgroup of membranes. *Chemistry and physics of lipids* **2013**, *175*, 84–91.

(70) Miguel, V.; Villarreal, M. A.; García, D. A. Effects of gabergic phenols on the dynamic and structure of lipid bilayers: A molecular dynamic simulation approach. *PloS one* **2019**, *14*, e0218042.

(71) Ahmad, S.; Johnston, B. F.; Mackay, S. P.; Schatzlein, A. G.; Gellert, P.; Sengupta, D.; Uchegbu, I. F. In silico modelling of drug–polymer interactions for pharmaceutical formulations. *Journal of the Royal Society Interface* **2010**, *7*, S423–S433.

(72) Gutierrez, A.; Atilhan, M.; Aparicio, S. Theoretical study on deep eutectic solvents as vehicles for the delivery of anesthetics. *The Journal of Physical Chemistry B* **2020**, *124*, 1794–1805.

(73) Van Der Spoel, D.; Lindahl, E.; Hess, B.; Groenhof, G.; Mark, A. E.; Berendsen, H. J. GROMACS: fast, flexible, and free. *Journal of computational chemistry* **2005**, *26*, 1701–1718.

(74) Abraham, M. J.; Murtola, T.; Schulz, R.; Páll, S.; Smith, J. C.; Hess, B.; Lindahl, E. GROMACS: High performance molecular simulations through multi-level parallelism from laptops to supercomputers. *SoftwareX* **2015**, *1*, 19–25.

(75) Vanommeslaeghe, K.; MacKerell Jr, A. D. Automation of the CHARMM General Force Field (CGenFF) I: bond perception and atom typing. *Journal of chemical information and modeling* **2012**, *52*, 3144–3154.

(76) Vanommeslaeghe, K.; Hatcher, E.; Acharya, C.; Kundu, S.; Zhong, S.; Shim, J.; Darian, E.; Guvench, O.; Lopes, P.; Vorobyov, I., et al. CHARMM general force field: A

force field for drug-like molecules compatible with the CHARMM all-atom additive biological force fields. *Journal of computational chemistry* **2010**, *31*, 671–690.

(77) Price, D. J.; Brooks III, C. L. A modified TIP3P water potential for simulation with Ewald summation. *The Journal of chemical physics* **2004**, *121*, 10096–10103.

(78) Hess, B.; Bekker, H.; Berendsen, H. J. C.; Fraaije, J. G. E. M. LINCS: A linear constraint solver for molecular simulations. *J. Comp. Chem.* **1997**, *18*, 1463–1472.

(79) Essmann, U.; Perera, L.; Berkowitz, M. L.; Darden, T.; Lee, H.; Pedersen, L. G. A smooth particle mesh Ewald method. *The Journal of chemical physics* **1995**, *103*, 8577–8593.

(80) Darden, T.; York, D.; Pedersen, L. Particle mesh Ewald: An N log (N) method for Ewald sums in large systems. *The Journal of chemical physics* **1993**, *98*, 10089–10092.

(81) Bussi, G.; Donadio, D.; Parrinello, M. Canonical sampling through velocity rescaling. *The Journal of chemical physics* **2007**, *126*, 014101.

(82) Bussi, G.; Zykova-Timan, T.; Parrinello, M. Isothermal-isobaric molecular dynamics using stochastic velocity rescaling. *The Journal of chemical physics* **2009**, *130*, 074101.

(83) Parrinello, M.; Rahman, A. Polymorphic transitions in single crystals: A new molecular dynamics method. *Journal of Applied physics* **1981**, *52*, 7182–7190.

(84) Nosé, S.; Klein, M. Constant pressure molecular dynamics for molecular systems. *Molecular Physics* **1983**, *50*, 1055–1076.

(85) Humphrey, W.; Dalke, A.; Schulten, K. VMD: visual molecular dynamics. *J. Mol. Graph.* **1996**, *14*, 33–8, 27–8.

(86) Rhys, N. H.; Gillams, R. J.; Collins, L. E.; Callear, S. K.; Lawrence, M. J.; McLain, S. E. On the structure of an aqueous propylene glycol solution. *The Journal of chemical physics* **2016**, *145*, 224504.

(87) Ferreira, E. S.; Voroshylova, I. V.; Koverga, V. A.; Pereira, C. M.; Cordeiro, M. N. D. New force field model for propylene glycol: insight to local structure and dynamics. *The Journal of Physical Chemistry B* **2017**, *121*, 10906–10921.

(88) Ghanadzadeh Gilani, A.; Akbarnia Dafrazi, A.; Rahmdel Delcheh, S.; Verpoort, F. Cyclopentanone–Alkanediol Systems: Experimental and Theoretical Study on Hydrogen-Bond Complex Formation. *Industrial & Engineering Chemistry Research* **2020**, *59*, 18318–18334.

(89) Chakraborty, S.; Kumar, H.; Dasgupta, C.; Maiti, P. K. Confined water: structure, dynamics, and thermodynamics. *Accounts of chemical research* **2017**, *50*, 2139–2146.

(90) Allen, M. P.; Tildesley, D. J. Computer Simulation of Liquids. **1987**,

(91) Ozkanlar, A. Structure of the Hydrogen-Bond Network in Binary Mixtures of Formamide and Methanol. *Journal of Solution Chemistry* **2021**, *50*, 257–276.

(92) Zhang, N.; Li, W.; Chen, C.; Zuo, J. Molecular dynamics simulation of aggregation in dimethyl sulfoxide–water binary mixture. *Computational and Theoretical Chemistry* **2013**, *1017*, 126–135.

(93) McLain, S. E.; Soper, A. K.; Luzar, A. Investigations on the structure of dimethyl sulfoxide and acetone in aqueous solution. *The Journal of chemical physics* **2007**, *127*, 174515.

(94) Egorov, A. V.; Lyubartsev, A. P.; Laaksonen, A. Molecular dynamics simulation study

of glycerol–water liquid mixtures. *The Journal of Physical Chemistry B* **2011**, *115*, 14572–14581.

(95) Paul, W. B. Molecular dynamics simulation, elementary methods. By JM Haile, Wiley, Chichester 1992, 489 pp., hardcover,£ 47.50, ISBN 0-471-81966-2. 1993.

(96) Henao, A.; Salazar-Rios, J. M.; Guardia, E.; Pardo, L. C. Structure and dynamics of water plastic crystals from computer simulations. *J. Chem. Phys.* **2021**, *154*, 104501.

(97) Luzar, A.; Chandler, D. Structure and hydrogen bond dynamics of water–dimethyl sulfoxide mixtures by computer simulations. *The Journal of chemical physics* **1993**, *98*, 8160–8173.

(98) D. van der Spoel, P. J. v. M.; Berendsen, H. J. C. A systematic study of water models for molecular simulation: Derivation of water models optimized for use with a reaction field. *J. Chem. Phys.* **1998**, *108*, 10220–10230.

(99) Laage, D.; Hynes, J. T. On the molecular mechanism of water reorientation. *J. Phys. Chem. B* **2008**, *112*, 14230–14242.

(100) Kawasaki, T.; Kim, K. Spurious violation of the StokesâĂŞEinsteinâĂŞDebye relation in supercooled water. *Sci. Rep.* **2019**, *9*, 8118.

(101) F. Paesani, S. I.; Voth, G. A. Quantum effects in liquid water from an ab initio-based polarizable force field. *J. Chem. Phys.* **2007**, *127*, 074506.

(102) Mallik, B. S.; Chandra, A. An ab initio molecular dynamics study of the frequency dependence of rotational motion in liquid water. *J. Mol. Liq.* **2008**, *143*, 31–34.

(103) Bandyopadhyay, S.; Chakraborty, S.; Bagchi, B. Secondary Structure Sensitivity of Hydrogen Bond Lifetime Dynamics in the Protein Hydration Layer. *J. Am. Chem. Soc.* **2005**, *127*, 16660–16667.

(104) Luzar, A.; Chandler, D. Effect of Environment on Hydrogen Bond Dynamics in Liquid Water. *Phys. Rev. Lett.* **1996**, *76*, 928.

(105) Chowdhary, J.; Ladanyi, B. M. Hydrogen Bond Dynamics at the Water/Hydrocarbon Interface. *J. Phys. Chem. B* **2009**, *113*, 4045–4053.

(106) Stillinger, F. H.; Rahman, A. Improved simulation of liquid water by molecular dynamics. *J. Chem. Phys.* **1974**, *60*, 1545–1557.

(107) Rapaport, D. C. Hydrogen bonds in water. *Mol. Phys.* **1983**, *50*, 1151–1162.

(108) Luzar, A. Resolving the hydrogen bond dynamics conundrum. *J. Chem. Phys.* **2000**, *113*, 10663–10675.